2018

# Structure-Activity Studies Reveal the Molecular Basis for GABA(B)-Receptor Mediated Inhibition of High Voltage-Activated Calcium Channels by α-Conotoxin Vc1.1

Mahsa Sadeghi
*University of Wollongong*, msadeghi@uow.edu.au

Bodil B. Carstens
*University of Queensland*

Brid P. Callaghan
*University of Wollongong*, *University of Queensland*

James T. Daniel
*University of Queensland*

Han Shen Tae
*University of Wollongong*, hstae@uow.edu.au

***See next page for additional authors***

## Publication Details

Sadeghi, M., Carstens, B. B., Callaghan, B. P., Daniel, J. T., Tae, H., O'Donnell, T., Castro, J., Brierley, S. M., Adams, D. J., Craik, D. J. & Clark, R. J. (2018). Structure-Activity Studies Reveal the Molecular Basis for GABA(B)-Receptor Mediated Inhibition of High Voltage-Activated Calcium Channels by α-Conotoxin Vc1.1. ACS Chemical Biology, 13 (6), 1577-1587.

# Structure-Activity Studies Reveal the Molecular Basis for GABA(B)-Receptor Mediated Inhibition of High Voltage-Activated Calcium Channels by α-Conotoxin Vc1.1

**Abstract**

α-Conotoxins are disulfide-bonded peptides from cone snail venoms and are characterized by their affinity for nicotinic acetylcholine receptors (nAChR). Several α-conotoxins with distinct selectivity for nAChR subtypes have been identified as potent analgesics in animal models of chronic pain. However, a number of α-conotoxins have been shown to inhibit N-type calcium channel currents in rodent dissociated dorsal root ganglion (DRG) neurons via activation of G protein-coupled $GABA_B$ receptors ($GABA_BR$). Therefore, it is unclear whether activation of $GABA_BR$ or inhibition of α9α10 nAChRs is the analgesic mechanism. To investigate the mechanisms by which α-conotoxins provide analgesia, we synthesized a suite of Vc1.1 analogues where all residues, except the conserved cysteines, in Vc1.1 were individually replaced by alanine (A), lysine (K), and aspartic acid (D). Our results show that the amino acids in the first loop play an important role in binding of the peptide to the receptor, whereas those in the second loop play an important role for the selectivity of the peptide for the $GABA_BR$ over α9α10 nAChRs. We designed a cVc1.1 analogue that is >8000-fold selective for $GABA_BR$-mediated inhibition of high voltage-activated (HVA) calcium channels over α9α10 nAChRs and show that it is analgesic in a mouse model of chronic visceral hypersensitivity (CVH). cVc1.1[D11A,E14A] caused dose-dependent inhibition of colonic nociceptors with greater efficacy in ex vivo CVH colonic nociceptors relative to healthy colonic nociceptors. These findings suggest that selectively targeting $GABA_BR$-mediated HVA calcium channel inhibition by α-conotoxins could be effective for the treatment of chronic visceral pain.

**Disciplines**

Medicine and Health Sciences

**Publication Details**

Sadeghi, M., Carstens, B. B., Callaghan, B. P., Daniel, J. T., Tae, H., O'Donnell, T., Castro, J., Brierley, S. M., Adams, D. J., Craik, D. J. & Clark, R. J. (2018). Structure-Activity Studies Reveal the Molecular Basis for GABA(B)-Receptor Mediated Inhibition of High Voltage-Activated Calcium Channels by α-Conotoxin Vc1.1. ACS Chemical Biology, 13 (6), 1577-1587.

**Authors**

Mahsa Sadeghi, Bodil B. Carstens, Brid P. Callaghan, James T. Daniel, Han Shen Tae, Tracey O'Donnell, Joel Castro, Stuart Brierley, David J. Adams, David J. Craik, and Richard J. Clark

# Structure-activity studies reveal the molecular basis for $GABA_B$-receptor mediated inhibition of high voltage-activated calcium channels by α-conotoxin Vc1.1.

Mahsa Sadeghi[1], Bodil B. Carstens[2], Brid P. Callaghan[3], James T. Daniel[4], Han-Shen Tae[1], Tracey O'Donnell[5,6], Joel Castro[5,6], Stuart M. Brierley[5,6], David J. Adams[1], David J. Craik[2] and Richard J. Clark[4*].

[1] Illawarra Health and Medical Research Institute (IHMRI), University of Wollongong, Wollongong, NSW 2522, Australia.

[2]The University of Queensland, Institute for Molecular Bioscience, Brisbane, Qld 4072, Australia.

[3]Department of Anatomy & Neuroscience, University of Melbourne, Parkville, Victoria 3010, Australia

[4]The University of Queensland, School of Biomedical Sciences, Brisbane, Qld 4072, Australia.

[5]Visceral Pain Research Group, Human Physiology, Centre for Neuroscience, College of Medicine and Public Health, Flinders University, Bedford Park, South Australia, 5042, Australia.

[6]Centre for Nutrition and Gastrointestinal Diseases, Discipline of Medicine, University of Adelaide, South Australian Health and Medical Research Institute (SAHMRI), North Terrace, Adelaide, Southern Australia 5000, Australia.

Address correspondence to: Dr. Richard J Clark, The University of Queensland, School of Biomedical Sciences, Brisbane, QLD, 4072, Australia. Phone: +61 7 3365 1527. Fax: +61 7 3365 1766. Email: richard.clark@uq.edu.au

**Abbreviated title:** Molecular basis of calcium channel inhibition by Vc1.1

**Abstract**

α-Conotoxins are disulfide-bonded peptides from cone snail venoms and are characterized by their affinity for nicotinic acetylcholine receptors (nAChR). Several α-conotoxins with distinct selectivity for nAChR subtypes have been identified as potent analgesics in animal models of chronic pain. However, a number of α-conotoxins have been shown to inhibit N-type calcium channel currents in rodent dissociated dorsal root ganglion (DRG) neurons via activation of G protein-coupled GABA$_B$ receptors (GABA$_B$R). Therefore it is unclear whether activation of GABA$_B$R or inhibition of α9α10 nAChRs is the analgesic mechanism. To investigate the mechanisms by which α-conotoxins provide analgesia, we synthesised a suite of Vc1.1 analogues where all residues, except the conserved cysteines, in Vc1.1 were individually replaced by alanine (A), lysine (K) and aspartic acid (D). Our results show that the amino acids in the first loop play an important role in binding of the peptide to the receptor whereas those in the second loop play an important role for the selectivity of the peptide for the GABA$_B$R over α9α10 nAChRs. We designed a cVc1.1 analogue that is >8000-fold selective for GABA$_B$R-mediated inhibition of high voltage-activated (HVA) calcium channels over α9α10 nAChRs and show that it is analgesic in a mouse model of chronic visceral hypersensitivity (CVH). cVc1.1[D11A,E14A] caused dose-dependent inhibition of colonic nociceptors with greater efficacy in *ex vivo* CVH colonic nociceptors relative to healthy colonic nociceptors. These findings suggest that selectively targeting GABA$_B$R-mediated HVA calcium channel inhibition by α-conotoxins could be effective for the treatment of chronic visceral pain.

Keywords: conotoxin, calcium channels, GPCRs, GABA$_B$ receptor, chronic pain, analgesia

Conotoxins are disulfide-rich peptides from the venom of marine snails of the *Conus* genus. They range in size from 10 to 40 amino acids in length and have a compact structure that is stabilised by one or more disulfide bonds. The molecular targets of conotoxins include a range of membrane receptors and ion channels, many of which have a role in neurophysiological signalling pathways, including pain. The α-conotoxin family of conotoxins are defined, in part, by their pharmacological target, the nicotinic acetylcholine receptors (nAChRs), range in size from 11 to 16 residues and have a helical structure that is stabilised by two disulfide bonds in a CysI to CysIII and CysII to CysIV arrangement (Figure 1A). The amino acids between CysII and CysIII and CysIII and CysIV form two loops that vary in the number and type of amino acids, and it is the composition of these loops that confers the exquisite selectivity that α-contoxins have for specific subtypes of nAChRs.

Recently, a subset of α-conotoxins have been shown to inhibit high voltage-activated (HVA) calcium channel currents via activation of the $GABA_B$ receptor ($GABA_BR$) (Figure 1B) . $GABA_BRs$[1-3] are G protein-coupled receptors (GPCRs) for γ-aminobutyric acid (GABA), the main inhibitory neurotransmitter in the brain and are a promising target for the treatment of a range of neurological and psychiatric disorders, including pain, depression and drug addiction[4]. Activating presynaptic $GABA_BRs$ inhibits neurotransmitter release by reducing the HVA calcium channel currents[5] that control neurotransmitter and hormone release, and which are key mediators in pain signal transmission in nociceptive neurons[6, 7]. Therefore, inhibiting HVA calcium channel currents either directly with selective antagonists or indirectly via GPCR modulation causes analgesia in animals and humans[8]. Vc1.1 was the first α-conotoxin shown to inhibit HVA calcium channels via $GABA_BR$ activation. This peptide was

discovered from a cDNA screen of the venom duct of the Western Australian cone snail *Conus victoriae*[9]. Testing for antagonist activity against a range of nAChR subtypes revealed that Vc1.1 was a selective inhibitor of the α9α10 nAChR subtype[10, 11]. However, it was subsequently shown that Vc1.1 and the α9α10 nAChR-selective α-conotoxin RgIA[12] were both able to also potently inhibit HVA calcium channel currents in rat dorsal root ganglion (DRG) neurons and that this inhibition was dependent on $GABA_BR$ activation[13-15]. Based on this finding, a number of other α-conotoxins that were antagonists of the α9α10 nAChR subtype were screened for their ability to inhibit voltage-gated calcium channels (VGCCs) and several additional members of this subgroup, including PeIA and Vc1.2, were identified[16, 17]. More recently a sequence homology approach was used to identify further members of this subgroup[18]. Although initially it appeared that the HVA calcium channel inhibition was correlated with α9α10 nAChR subtype inhibition, a number of the more recently described HVA calcium channel inhibitory α-conotoxins, including AuIB, Vc1.2 and Pu1.2, are not antagonists of the α9α10 nAChR subtype[19].

The specific molecular mechanisms responsible for these α-conotoxin's analgesic effects *in vivo* has been controversial due to the identification of distinct pharmacological targets for these peptides. Therefore, deliniating the precise molecular mechanisms responsible for their analgesic effects *in vivo* is important. Although the α9α10 nAChR subtype was originally proposed to be the primary analgesic target of Vc1.1 and RgIA, several observations have cast doubt on its importance for α-conotoxin analgesia instead supporting a more prominent role of HVA calcium channel inhibition via $GABA_BR$ activation. Post-translationally modified Vc1.1 analogues, vc1a and [P6O]Vc1.1, which are α9α10 antagonists but lack activity at $GABA_BR$, do not

produce analgesia in *ex vivo* or *in vivo* assays[20, 21], However, α-conotoxins which are inactive at α9α10 but active at $GABA_BR$, namely AuIB and a truncated loop 1 analogue of Vc1.1, are analgesic in rodent models of mechanical allodynia and visceral hypersensitivity, respectively[18, 19]. Moreover, blockade of $GABA_BR$ activity by pre-treatment with selective antagonists CGP55845 or SCH50911 suppresses the analgesic effects of α-conotoxins in multiple different rodent pain models (partial nerve ligation (PNL), chronic constriction injury (CCI), and CVH)[19, 21, 22]. Conversely, other evidence supports the alternative hypothesis that α9α10 inhibition is the primary analgesic mechanism. A recently developed analogue of RgIA, called RgIA4, which is highly selective for α9α10 inhibition but has been reported to have no effect on $GABA_BR$ or calcium channels, reduces mechanical hyperalgesia and cold allodynia in an oxaliplatin-induced neuropathic pain model[23]. Furthermore, selective small molecule α9α10 nAChR antagonists ZZ-204G and ZZ1-61c are also analgesic in rodent models of mechanical hyperalgesia[24, 25]. In light of these conflicting hypotheses, interrogating the relative contribution of nAChR inhibition and HVA calcium channel inhibition toward α-conotoxin analgesia is essential for their continued development as therapeutics.

To develop these conotoxins as potential analgesics it is important to identify the key peptide residues for the interaction with both the α9α10 nAChR and the $GABA_BR$. A comprehensive structure-activity study of Vc1.1 at the α9α10 nAChR, where an alanine, lysine and aspartic acid scan was performed, revealed that key regions in Vc1.1 for activity were residues Asp5-Asp7 and Asp11-Ile15.[26] Selective mutants of Vc1.1 at position 4 and 9 had enhanced potency at the α9α10 nAChR.[26] A subsequent modelling study using this structure-activity data and additional peptide mutants showed that Vc1.1 preferentially bound to the α10α9 binding pocket rather than to the α9α10

interface and also identified a key interaction to explain the difference in affinity of Vc1.1 for the rat vs human homologues of the nAChR.[27] Substantial structure-activity studies have also been undertaken to investigate the molecular determinants of the interaction between RgIA and the α9α10 nAChR.[28, 29] These findings have ultimately led to the recent development of the potent and selective α9α10 nAChR selective analgesic analogue RgIA4.

To further clarify the roles of the α9α10 nAChR and HVA calcium channel inhibition on the analgesic effects of this sub-family of α-conotoxins, we undertook a systematic study of the structure-activity relationships of Vc1.1 inhibition of HVA calcium channel currents. Using this data, we designed and synthesized a Vc1.1 analogue that is >8000-fold selective for $GABA_BR$-mediated inhibition of HVA calcium channels over α9α10 nAChRs. Finally, we show that this peptide was able to induce a dose-dependent inhibition of colonic nociceptors with greater efficacy in a mouse model of chronic visceral hypersensitivity (CVH), demonstrating its analgesic properties.

## Results and Discussion

### Activity of Vc1.1 analogues on HVA calcium channels current in DRG neurons:

We previously described the synthesis, structural characterisation and α9α10 nAChR inhibition of alanine, aspartic acid and lysine scan mutants of Vc1.1.[26] This panel of mutants allows us to determine the effect of successively replacing the non-cysteine residues in Vc1.1 with "inert" (alanine), negatively charged (aspartic acid) or positively charged (lysine) amino acids on biological activity. Therefore our approach in this study was to investigate the functional activity of this panel of Vc1.1 analogues

for their effect on HVA calcium channel currents in acutely isolated neurons from mouse or rat dorsal root ganglia (DRG). NMR structural analysis of the P13A, P13D, P6K and P13K mutants of Vc1.1 revealed structural pertubations, presumably due to replacement of structurally important proline residues, so the changes in biological activity of these peptides is likely due to a change in the backbone conformation of each peptide rather than alteration of the specific sidechain functionality.[26] All Vc1.1 analogues were screened at a single concentration of 100 nM upon activation of HVA calcium channel currents in DRG neurons. The pooled data for all of the mutants for the single point screen are summarized in Figure 2 and the results were statistically analysed using a two-tailed student *t* test. Alanine substitution (Figure 2A) at position $Gly^{1}$, $Asp^{11}$, $Glu^{14}$ and $Ile^{15}$ of Vc1.1 did not change Vc1.1 inhibition of HVA calcium channel current (30.1 ± 1.3% (*n* = 4), 36.9 ± 3.8% (*n* = 11), 29.9 ± 2.7% (*n* = 5) and 26.8 ± 1.4% (*n* = 4) inhibition, respectively). However, alanine substitution at other residues resulted in loss of inhibitory activity on HVA calcium channels in mice DRG neurons. Representative traces of HVA calcium channel inhibition in mice DRG neurons by Vc1.1 analogues equipotent to Vc1.1 and less effective than Vc1.1 are shown in Figure S2A. The alanine scan mutants of Vc1.1 were also tested for inhibitory activity on HVA calcium channels in rat DRG neurons and similar results were obtained (Figure S1). In cells showing HVA calcium channel current ($I_{Ba}$) inhibition in response to α-conotoxin exposure, subsequent application of baclofen (50 μM) suppressed $I_{Ba}$ further depending on the tested analogues. The data show that there is a significant difference between the $I_{Ba}$ inhibition by baclofen (50 μM) (43.2 ± 0.8%; *n* = 127) and Vc1.1 (31.4 ± 3.2%; *n* = 9). However, there is no significant difference between the $I_{Ba}$ inhibition by D11A (36.9 ± 3.8%) compared to baclofen. Concentration-response data for inhibition of $I_{Ba}$ in rat DRG neurons by Vc1.1 and

alanine substituted active analogues of Vc1.1 namely, G1A, D11A, E14A and I15A confirms these results (Figure S1B). Although the estimated $IC_{50}$ for these analogues (13.1, 6.8, 23.1 and 170.7 nM, respectively) are similar to that of Vc1.1 (2.5 nM), the maximum inhibition of $I_{Ba}$ at 100 nM concentration of these peptides is greater than those with Vc1.1, highlighting that the efficacy of these peptides is greater on inhibiting $I_{Ba}$ in DRG neurons.

The pooled data for aspartic acid substituted mutants tested at 100 nM are summarized in Figure 2B. Aspartic acid substitution at position $Gly^{1}$, $Ser^{4}$, $Asn^{9}$, $Glu^{14}$, $Ile^{15}$ retained activity at $GABA_BR$ inhibition of HVA calcium channel currents (33.1 ± 4.2% (n = 5), 23.8 ± 3.7% (n = 8), 25.7 ± 2.3% (n = 9), 32.7 ± 3.8% (n = 3) and 25.4 ± 5.4% (n = 5) inhibition, respectively). However, aspartic acid substitution at other residues resulted in loss of activity on HVA calcium channels in mice DRG neurons. Representative traces of $I_{Ba}$ inhibition in mice DRG neurons by Vc1.1 analogues equipotent and less potent to Vc1.1 are shown in Figure S2B. There was also no significant difference observed between $I_{Ba}$ inhibition by E14D (32.7 ± 3.8%) compare to 50 μM baclofen (43.2 ± 0.8%).

Finally, the pooled data for lysine substituted mutants tested at 100 nM are summarized in Figure 2C. Lysine substitution at position $Ser^{4}$, $Asn^{9}$, $Asp^{11}$ produced comparable inhibitory activities at HVA calcium channels to Vc1.1. (24.8 ± 3.6% (*n* = 8), 23.8 ± 2.7% (*n* = 7) and 39.1 ± 4.1% (*n* = 6) inhibition of $I_{Ba}$, respectively). In addition, there was no significant difference between $I_{Ba}$ inhibition by Vc1.1[D11K] (39.05 ± 4.1%) compared to baclofen (50 μM) (43.2 ± 0.8%). However, lysine substitution at other residues results in loss of activity on HVA calcium channels in

mice DRG neurons. Representative traces of $I_{Ba}$ inhibition in mice DRG neurons by Vc1.1 analogues equipotent to and less potent to Vc1.1 are shown in Figure S2C.

Figure 2D summarises the structure-activity relationships for Vc1.1 inhibition of HVA calcium channel currents and ACh-evoked currents mediated by α9α10 nAChRs.[26] Overall, the results indicate that subsititutions in loop 2 of Vc1.1 are better tolerated for HVA calcium channel inhibition compared to α9α10 nAChR inhibition as mutations at positions 9, 11, 14 and 15 generally do not cause a significant loss in activity. This finding is consistent with our recent study that indicated the key bioactive epitope for $GABA_BR$-targeting conotoxins was focused around loop 1 of Vc1.1.[18] The importance of both loops for α9α10 nAChR inhibition by α-conotoxins is further supported by the structure-activity studies on RgIA, which have shown that mutations in both loops can have significant impact on potency.[23, 28] Additionally, this is supported by modelling studies of the interaction of both RgIA and Vc1.1 with the α9α10 nAChR.[27, 30] Therefore, the difference in the importance of the loop sequences on biological activity suggests that introducing a combination of mutations into loop 2 of Vc1.1 should result in an analogue that is highly selective for $GABA_BR$-mediated HVA calcium channel inhibition over α9α10 nAChR inhibition.

**Design of a selective Vc1.1 inhibitor of $GABA_BR$-mediated HVA calcium channels.**

Given that Vc1.1 and RgIA have been shown to inhibit both α9α10 nAChRs and $GABA_BR$-mediated HVA calcium currents, the challenge has been to determine the contribution of these two mechanisms to the analgesic effects of these peptides. We have previously shown that substitution of $Pro^6$ in Vc1.1 with hydroxyproline

abolishes HVA calcium channel inhibition in rat DRG neurons and that this analogue is neither analgesic in the rat partial nerve ligation model of neuropathic pain[20] nor inhibits colonic nociceptors from CVH mice.[21] Furthermore, inhibition of colonic nociceptors by Vc1.1 could be antagonized by the selective $GABA_BR$ antagonist CGP55845.[21] These results suggest that $GABA_BR$-dependant HVA calcium channel inhibition underlies the analgesic effects of Vc1.1. However, RgIA analogues selective for only α9α10 nAChR inhibition have been shown to be effective in animal models of chemotherapy-induced neuropathic pain.[23] Therefore, to clarify the mechanism of analgesic action, we used the structure-activity relationships determined from this study and our previous work[26] to design a Vc1.1 analogue that was a potent and selective inhibitor of the $GABA_BR$-dependant HVA calcium channels.

As described above, mutation of either $Asp^{11}$ or $Glu^{14}$ in Vc1.1 resulted in no change in potency for HVA calcium channel inhibition. However, these individual Vc1.1 mutations substantially reduced inhibition of α9α10 nAChRs[26] and modelling of the interaction between Vc1.1 and α9α10 predicted that Asp11 and Glu14 form key salt bridge interactions with arginine residues on the α9α10 nAChR.[27] Furthermore, during our previous development of an orally active, backbone cyclised analogue of Vc1.1, we observed a five-fold decrease and 12-fold increase in potency for α9α10 nAChR and HVA calcium channel inhibition, respectively, when Vc1.1 was cyclised.[31] Therefore, we chose to synthesize two analogues, the Vc1.1 double mutant, Vc1.1[D11A,E14A], and its corresponding cyclic analogue, cVc1.1[D11A,E14A], and characterised their ability to selectively inhibit HVA calcium channel currents.

Vc1.1[D11A,E14A] was successfully synthesized using FMOC-based solid phase peptide synthesis and the cyclic analogue was produced using BOC-based solid phase peptide synthesis utilising a C-terminal thioester to facilitate an intramolecular native chemical ligation reaction to form the cyclic backbone. Both peptides were characterised by NMR spectroscopy and Hα chemical shift analysis indicated that the structures of Vc1.1[D11A,E14A] and cVc1.1[D11A,E14A] were consistent with the native sequences (Figure S3, Table S1). To confirm this we determined the three dimensional structure of cVc1.1[D11A,E14A]. Structures were calculated in CYANA 3.0 [32] using NOE-derived distance restraints and TALOS-N[33] derived dihedral angle restraints. The structural statistics for the ensemble of the 20 lowest energy structures for cVc1.1[D11A,E14A] are shown in Table S2 and the structural ensemble overlayed over the backbone atoms from Cys2 to Cys16 (rmsd = 0.21 ± 0.11 Å) is shown in Figure 3A. The atomic coordinates have been deposited in the Protein Data Bank (PDB ID 6CGX). The three-dimensional structure of cVc1.1[D11A,E14A] is consistent with that of Vc1.1 and other α-conotoxins, comprising of an α-helical region from Pro6 to Ala11 that is cross-braced by the two disulfide bonds (Figure 3B). There is also some helical character in the linker region of the cyclic peptide, which has been observed in other cyclised α-conotoxins.[34] Figure 3C shows a comparison of the surface features of cVc1.1 and cVc1.1[D11A,E14A], illustrating that both peptides are similar except for the absence of a patch of negatively charged residues formed by Asp11 and Glu14 in Vc1.1. Finally, a comparison of the lowest energy structures of cVc1.1 and cVc1.1[D11A, E14A] reveals that the amide backbones of the two peptides adopt a similar conformation (Figure 3D).

Both Vc1.1[D11A,E14A] and cVc1.1[D11A,E14A] were tested for their ability to inhibit HVA calcium channel currents in mice DRG neurons (Figure 4A) and ACh-evoked currents of human α9α10 nAChRs heterologously expressed in *Xenopus* oocytes (Figure 4B). At 100 nM, Vc1.1[D11A,E14A] and cVc1.1[D11A,E14A] inhibited HVA calcium channel current amplitude by 38.4 ± 2.5% ($n$ = 7) and 48.9 ± 4.7% ($n$ = 7), respectively (Figure 4A(i)). The efficacy of cVc1.1[D11A,E14A] was also significantly greater at inhibiting HVA calcium channel current than Vc1.1 (30.4± 3.2%) at 100 nM (Figure 4A(ii)). Concentration-response relationships revealed that Vc1.1[D11A, E14A] and cVc1.1[D11A, E14A] are equipotent at inhibiting HVA calcium currents in mice DRG neurons with $IC_{50}$ values of 2.5 ± 1.1 and 3.3 ± 1.1 nM, respectively (Figure 4A(iii)), which is comparable to Vc1.1 (1.7 nM) but slightly less than cVc1.1 (0.3 nM).[13, 22] Interestingly, although backbone cyclisation appears to have improved the efficacy of the Vc1.1[D11A, E14A], no improvements in potency were observed as was the case for native Vc1.1.

Vc1.1[D11A, E14A] and cVc1.1[D11A, E14A] were also assessed for their ability to inhibit ACh-evoked currents in *Xenopus* oocytes expressing hα9α10 nAChRs. Both Vc1.1 analogues tested at a concentration of 1 μM were significantly less potent at inhibiting the ACh-evoked currents (3.0 ± 2.6%, $n$ = 7 and 6.4 ± 2.9%, $n$ = 9, respectively) than the native peptide, Vc1.1, (64.0 ± 3.5% $n$ = 6) (Figure 4B). Both Vc1.1.[D11A,E14A] and cVc1.1[D11A, E14A] inhibited the ACh-evoked currents in a concentration-dependent manner with $IC_{50}$'s of 9.2 ± 1.3 μM and 29.3 ± 3.0 μM, respectively. Moreover, cVc1.1[D11A, E14A] was also tested at rat α9α10 nAChRs expressed in *Xenopus* oocytes (Figure S4) with comparable potency to that at hα9α10 nAChRs ($IC_{50}$ = 17.9 ± 2.6 μM, n = 3-8). Therefore, as predicted from the mutational

data, introduction of the two alanine mutations caused a significant reduction in potency, which was further reduced by introduction of the cyclic backbone. Overall, Vc1.1[D11A,E14A] and cVc1.1[D11A, E14A] were 3,700-fold and 8,800-fold more selective for HVA calcium channel inhibition over inhibition of α9α10 nAChRs, respectively. This substantial selectivity for HVA calcium channel inhibition suggests that cVc1.1[D11A, E14A] is an excellent molecule for investigating the role of this pathway in the analgesic action of Vc1.1.

**Anti-nociceptive actions of cVc1.1[D11A, E14A] in an animal model of chronic visceral pain.**

We have previously shown that the anti-nociceptive actions of Vc1.1 can be inhibited by a selective $GABA_BR$ antagonist, whereas a Vc1.1 analogue inactive at $GABAB_R$ failed to inhibit of colonic nociceptors.[21] Therefore, we sought to investigate the anti-nociceptive effects of cVc1.1[D11A,E14A], which is selective only for the $GABA_BR$ in a mouse model of CVH. cVc1.1[D11A,E14A] caused dose-dependent inhibition of *ex vivo* colonic nociceptors from healthy (Figure 5A) and CVH (Figure 5B) mice. Notably, cVc1.1[D11A,E14A] caused greater inhibition of CVH colonic nociceptors relative to healthy colonic nociceptors (Figure 5C, 5D, 5E). We have shown previously that cVc1.1 has anti-nociceptive actions, with greater efficacy in a model of CVH [35]. Here we present this data as a percentage change in baseline in both the healthy and CVH states (Figure 5F) and also demonstrate that cVc1.1[D11A,E14A] has a greater inhibitory effect in CVH states compared with healthy states (Figure 5G). A direct comparison of anti-nociceptive efficacy of cVc1.1 and cVc1.1[D11A,E14A] shows that both peptides cause a similar levels of inhibition in the respective healthy (Figure 5H) and CVH states (Figure 5I). Given that both cVc1.1 and cVc1.1[D11A,E14A] cause a

similar level of inhibition in healthy control states, this implicates the involvement of $GABA_BR$ activation in the anti-nociceptive action. Whilst both cVc1.1 and cVc1.1[D11A,E14A] cause greater inhibition of colonic nociceptors in CVH states compared with healthy states, they evoke equivalent inhibition in CVH states, again implicating $GABA_BR$ activation in this anti-nociceptive action. We have previously shown an increased expression of $Ca_V2.2$ within colon-innervating DRG neurons from CVH mice,[21] which is likely to explain the enhanced anti-nociceptive actions of both cVc1.1 and cVc1.1[D11A,E14A] following $GABA_BR$ activation.

**Conclusion**

A subset of α-conotoxins, including Vc1.1 and RgIA, are thought to produce their pain relieving effects by inhibiting either nicotinic acetylcholine receptors or HVA calcium channels via $GABA_BR$ activation in mammalian sensory neurons. By demonstrating that an α-conotoxin analogue selective for $GABA_BR$ mediating HVA calcium channel inhibition is analgesic in a mouse model of chronic visceral pain, this study provides compelling evidence for the role of this analgesic mechanism. This finding opens novel perspectives in the pharmacological intervention of chronic pain management and the potential use of $GABA_BR$-targeting α-conotoxins as treatments for chronic pain conditions.

## Methods

### *Peptide synthesis*

All of the linear peptides were synthesised and characterised as described previously.[26] The cyclic analogue cVc1.1[D11A,E14A] was synthesised on PAM-Gly-Boc (Novabiochem) resin by manual solid phase peptide synthesis using with an *in situ* neutralization/2-(1H-benzotriazol-1-yl)-1,1,3,3-tetramethyluronium hexafluorophosphate activation procedure for Boc (*t*-butoxycarbonyl) chemistry.[36] A thioester moiety was incorporated at the C-terminus of the peptide as described previously [31] to allow cyclisation by intramolecular native chemical ligation[37] post-cleavage. The side chains of Cys3 and Cys14 were protected with acetamidomethyl (Acm) to facilitate regioselective disulfide formation. The peptide was cleaved from the resin by incubation in anhydrous HF containing *p*-cresol (5%) as a scavenger for 90 minutes at 0 – 5 $^{o}$C. The HF was then removed under vacuum, the peptide by precipitated by addition of cold diethyl ether and then collected by filtration. The peptide was then redissolved in 50% buffer A/B (A: $H_2O$ with 0.05% trifluoroacetic acid; B: 90% acetonitrile, 10% $H_2O$, 0.045% trifluoracetic acid) and lypholised. Purification of the linear reduced peptide was achieved using RP-HPLC as described for the linear peptides. The backbone cyclisation and formation of the Cys2-Cys8 disulfide bond was then formed in one step by incubation of the peptide in 0.1M $NH_4HCO_3$ (pH 8.2) at a concentration of 0.3 mg/mL overnight at room temperature. The peptide was then purified by RP-HPLC to yield the cyclised peptide containing a single disulfide bond. Formation of the Cys3-Cys16 disulfide bond was achieved by dissolving the peptide in 20% aqueous acetic acid and then adding saturated iodine solution (in 20% aqueous acetic acid) dropwise until the solution was pale yellow.

The mixture was stirred overnight at room temperature and then the reaction quenched by addition of a solution of 1M ascorbic acid until the solution became colourless. The peptide was then purified by RP-HPLC and the purity and identity of the peptide was confirmed by analytical RP-HPLC and ESMS analysis.

***NMR spectroscopy***

NMR data for Vc1.1[D11A,E14A] and cVc1.1[D11A,E14A] were measured as described previously.[26] Briefly, peptides were dissolved in 90% $H_2O$/10% $D_2O$ (pH 3.5 – 4.0) and two-dimensional NMR TOCSY and NOESY experiments recorded at 280 K on a Bruker Avance 600 NMR spectrometer. Spectra were analyzed using Topspin 1.3 (Bruker) and Sparky software.

***In vitro biological activity***

*Dorsal root ganglion (DRG) neuron preparation and culture:* Mice and rats were euthanized with isoflurane inhalation followed by decapitation and rats were killed by cervical dislocation, as approved by the Wollongong University Animal Ethics Committee. Thoracic and lumbar DRG neurons were collected, digested, and mechanically triturated from ganglia of 8-10 week-old C57BL/6 mice or 4-16 day-old Wistar rats as described previously[13, 38]. Cell suspensions were washed twice in supplemented DMEM (containing 10% heat-inactivated FBS and 1% penicillin/streptomycin) (Thermo Fisher Scientific), resuspended in supplemented DMEM and plated on poly-D-lysine/laminin-coated 12 mm round coverslips (BD Biosciences, Bedford, MA, USA), incubated at 37°C in high relative humidity (95%) and controlled $CO_2$ level (5%), and used within 16–36 h.

*In vitro cRNA synthesis, oocyte preparation and microinjection:* Plasmid pT7TS constructs of human α9 and α10 nAChR subunits were linearized with *XbaI* restriction enzyme New England Biolabs, Ipswich, MA, USA) for *in vitro* cRNA transcription using the T7 mMessage mMachine transcription kit (AMBION, Forster City, CA, USA).

Stage V-VI oocytes (1200-1300 μm in diameter) were obtained from *Xenopus laevis*, defolliculated with 1.5 mg/ml collagenase Type II (Worthington Biochemical Corp., Lakewood, NJ, USA) at room temperature (20-24 °C) for 1-2 h in OR-2 solution containing (in mM) 82.5 NaCl, 2 KCl, 1 $MgCl_2$ and 5 HEPES at pH 7.4. Oocytes were injected with 35 ng of human α9α10 nAChR cRNA (concentration confirmed spectrophotometrically and by gel electrophoresis) using glass pipettes pulled from glass capillaries (3-000-203 GX, Drummond Scientific Co., Broomall, PA, USA). Oocytes were incubated at 18ºC in sterile ND96 solution composed of (in mM) 96 NaCl, 2 KCl, 1 $CaCl_2$, 1 $MgCl_2$ and 5 HEPES at pH 7.4, supplemented with 5 % FBS, 0.1 mg/L gentamicin (GIBCO, Grand Island, NY, USA) and 10000 U/mL penicillin-streptomycin (GIBCO, Grand Island, NY, USA). All procedures were approved by the University of Sydney Animal Ethics Committee.

*Electrophysiological recordings:* Depolarization-activated membrane currents through high voltage-activated (HVA) calcium channels in rodent DRG neurons were recorded in the whole-cell recording configuration of the patch clamp technique with an Axopatch 700B amplifier (Molecular Devices Corp., Sunnyvale, CA) at room temperature (22-24°C). DRG neurons were transferred into a small volume (< 200 μl) recording chamber, which was constantly perfused with an extracellular (bath)

solution containing (in mM): 150 TEA-Cl, 2 $BaCl_2$, 10 D-glucose and 10 HEPES, pH 7.4 using a gravity-fed perfusion system at a flow rate of ~1 ml/min. Fire-polished borosilicate (C150TF-7.5, Harvard Apparatus Ltd.) patch pipettes with tip resistance values of 1.5–2.2 MΩ were filled with an intracellular solution containing (in mM): 140 CsCl, 1 $MgCl_2$, 4 MgATP, 0.1 Na-GTP, 5 1,2-bis(O-aminophenoxy)ethane-N,N,N′,N′-tetraacetic acid tetracesium salt (BAPTA)-$Cs_4$, and 10 HEPES-CsOH, pH 7.3. A voltage protocol using step depolarization from −80 to −10, −5 , 0 or +5 mV was used when examining HVA calcium channel current. Currents were generated by a computer using pCLAMP 10 software (Molecular Devices Corp) and depolarization-activated $Ba^{2+}$ currents ($I_{Ba}$) were filtered at 3 kHz and sampled at 10 kHz. Leak and capacitive currents were subtracted using a −P/4 pulse protocol. Depolarization-activated $Ba^{2+}$ peak current amplitude values ($I/I_{control}$) were determined from current amplitudes recorded at steady state in the absence ($I_{control}$) and presence of α-conotoxin (I).

Electrophysiological recordings in oocytes were carried out 2–5 days post cRNA microinjection. Two-electrode voltage clamp recordings of *X. laevis* oocytes expressing human α9α10 nAChRs were performed at room temperature using a GeneClamp 500B amplifier and pClamp 9 software interface (Molecular Devices, Sunnyvale, CA, USA) at a holding potential −80 mV. Voltage-recording and current-injecting electrodes were pulled from GC150T-7.5 borosilicate glass (Harvard Apparatus, Holliston, MA, USA) giving resistances of 0.3–1 MΩ when filled with 3 M KCl.

Oocytes were incubated in 100 μM BAPTA-AM ~3 h before recording and perfused with ND115 solution containing (in mM): 115 NaCl, 2.5 KCl, 1.8 $CaCl_2$, and 10 HEPES at pH 7.4 using a continuous Legato 270 push/pull syringe pump perfusion system (KD Scientific, Holliston, MA, USA) at a rate of 2 ml/min.. Due to the $Ca^{2+}$ permeability of hα9α10 nAChRs, BAPTA-AM incubation was carried out to prevent the activation of *X. laevis* oocyte endogenous $Ca^{2+}$-activated chloride channels.

Initially, oocytes were briefly washed with ND115 solution followed by three applications of acetylcholine (ACh) at half-maximal effective concentration ($EC_{50}$) of 6 μM for hα9α10 nAChR. Washout with ND115 solution was done for 3 min between ACh applications. Oocytes were incubated with peptide for 5 min with the perfusion system turned off, followed by co-application of ACh and peptide with flowing ND115 solution. All peptide solutions were prepared in ND115 + 0.1% bovine serum albumin. Peak current amplitudes before (ACh alone) and after (ACh + peptide) peptide incubation were measured using Clampfit version 10.7.0.3 software (Molecular Devices, Sunnyvale, CA, USA), where the ratio of ACh + peptide-evoked current amplitude to ACh alone-evoked current amplitude was used to assess the activity of the peptides at hα9α10 nAChR.

*Statistical analysis:* Data are mean ± SEM (n, number of experiments). Statistical analyses were performed in Prism 7 (Graphpad software, La Jolla, CA, USA) using Student's t test for two groups or one-way ANOVA with Bonferroni post hoc testing when appropriate. Differences were considered statistically significant at $P < 0.05$. The $IC_{50}$ was determined from concentration-response curve fitted to a non-linear regression function and reported with error of the fit.

***In vivo biological activity***

*Animals:* The Animal Ethics Committees of the South Australian Health and Medical Research Institute (SAHMRI) and Flinders University approved experiments involving animals. Male C57BL/6J mice aged 13-17 weeks of age were used in all experiments. Mice were acquired from an in-house C57BL/6J breeding program within SAHMRI's opportunistic and specific pathogen free animal care facility.

Mice were group housed (5 mice per cage) within individual ventilated cages (IVC), which were filled with aspen wood chip bedding (CA PURA CHIP ASPEN COARSE (Cat#-ASPJMAEB). These cages were stored on IVC racks in specific housing rooms within a temperature controlled environment of 22°C and a 12 hr light/ 12 hr dark cycle. Mice were feed at libitum with Jackson lab diet: 5K52 JL RAT & MOUSE/AUTO 6F DIET (Cat# - ASSPECIAL) and reverse osmosis purified water (EcoPure, UK). IVC cages contained Jackson lab bedding: CA PURA CHIP ASPEN COARSE (Cat# - ASPJMAEB). Mice had an average weight of ~ 29 g on the experimental day. Mice were randomly assigned to healthy control or trinitrobenzene sulphonic acid (TNBS) treatment groups. Following TNBS administration, mice were individually housed in individual ventilated cages to allow for accurate clinical monitoring until the experimental day in question. Mice were randomly assigned to study sub-groups, whilst the order of treatment was also randomised. Where possible, investigators were blinded to either the drugs being administered or during analysis the treatment group.

*Model of chronic visceral hypersensitivity (CVH):* Colitis was induced by administration of TNBS as described previously.[21, 39-43] Briefly, 13-week-old mice,

anaesthetized with isofluorane, were administered an intracolonic enema of 0.1mL TNBS (135 μL/mL of 1M solution in 35% ethanol), via a polyethylene catheter inserted 3 cm from the anus. Mice were then individually housed and observed daily for changes in body weight, physical appearance and behaviour. Previous studies using this model showed mucosal architecture, cellular infiltrate, crypt abscesses, and goblet cell depletion confirming TNBS induces significant damage to the colon by day 3-post treatment. This damage largely spontaneously recovers by day 7 and is fully resolved by day 28. At the 28-day time point, the high-threshold nociceptors in these mice display significant mechanical hypersensitivity and lower mechanical activation thresholds [41]. Increased neuronal activation in the dorsal horn of the spinal cord in response to noxious colorectal distension, as well as sprouting of colonic afferent terminals within the dorsal horn has also been reported.[44] The model also induces hyperalgesia and allodynia to colorectal distension,[45] and is termed Chronic Visceral Hypersensitivity (CVH).[21, 39-43]

*Ex-vivo single fibre colonic splanchnic afferent recording preparation:* Mice were humanely killed, by $CO_2$ inhalation at days 0 (healthy), and 28 (CVH) after TNBS administration. The colon and rectum (5–6 cm) and attached splanchnic nerves were removed and afferent recordings from splanchnic nerves were performed as described previously.[41, 46, 47] Briefly, colons were removed, split open and pinned flat, mucosal side up, in a specialized organ bath. The colonic compartment was superfused with a modified Krebs solution (in mM: 117.9 NaCl, 4.7 KCl, 25 $NaHCO_3$, 1.3 $NaH_2PO_4$, 1.2 $MgSO_4 (H_2O)_7$, 2.5 $CaCl_2$, 11.1 D-glucose), bubbled with carbogen (95% $O_2$, 5% $CO_2$) at a temperature of 34°C. All solutions contained the L-type calcium channel antagonist nifedipine (1 μM) to suppress smooth muscle activity and the

prostaglandin synthesis inhibitor indomethacin (3 μM) to suppress potential inhibitory actions of endogenous prostaglandins. The nerve bundle was extended into a paraffin-filled recording compartment in which finely dissected strands were laid onto a mirror, and single fibres placed on the platinum recording electrode. Action potentials, generated by mechanical stimuli to the colon's receptive field, were recorded by a differential amplifier (A-M Systems, Inc. Model 3000), filtered and sampled (20 kHz) using a 1401 interface (Cambridge Electronic Design, Cambridge, UK) and stored on a PC for off-line analysis.

*Colonic afferent classification and selection:* Receptive fields were identified by systematically stroking the mucosal surface with a still brush to activate all subtypes of mechanoreceptors. Categorization of afferents properties was in accordance with our previously published classification system.[46, 47] Once identified, receptive fields were tested with three distinct mechanical stimuli to enable classification: static probing with calibrated von Frey hairs (vfh) (2 g force; applied 3 times for a period of 3 sec), mucosal stroking with calibrated vfh (10 mg force; applied 10 times) or circular stretch (5 g; applied for a period of 1 min). We tested the effect of cVc1.1[D11A,E14A] on serosal afferents, also termed vascular afferents, recorded from the splanchnic pathway. These colonic afferents have high-mechanical activation thresholds and respond to noxious distension (40 mmHg), stretch (≥7 g) or vfh filaments (2 g) but not to fine mucosal stroking (10 mg vfh).[21, 40, 43, 46, 48] The algesic ion channels and receptors, $Na_V1.1$[43], TRPV1[47], TRPA1[49, 50], TRPV4[51], $P2X_3$[47] are highly expressed in these afferents. In addition, serosal afferents become mechanically hypersensitive in models of chronic visceral pain and have a nociceptor phenotype.[18, 21, 39, 40, 43, 46] In the present study, they are therefore referred to as colonic 'nociceptors'.

*Peptide application to colonic afferents:* Peptides were prepared from stock solutions, diluted to appropriate final concentrations in Krebs solution, and applied via a small metal ring placed over the afferent receptive field of interest. Once baseline splanchnic colonic nociceptor responses had been established, mechanosensitivity was re-tested after application of cVc1.1[D11A,E14A] (1, 10, 100, 1000 nM). Each concentration of the peptide was applied to the mucosal surface of the colon for 5 minutes as described previously.[18, 21, 39, 40, 43]

*Statistical analysis of afferent recording data:* Action potentials were analysed off-line using the Spike 2 (version 5.21) software (Cambridge Electronic Design, Cambridge, UK) and discriminated as single units based on distinguishable waveforms, amplitudes and durations. Data are expressed as mean ± SEM. *n* indicates the number of individual afferents. In some instances, data are presented as 'percentage change from baseline'. This is calculated by determining the change in mechanosensitivity of individual afferents between the normal 'baseline' response in healthy or CVH conditions compared to the respective mechanical responses following peptide addition. This difference is then averaged across all afferents with a cohort to obtain a final mean ± SEM and converted to a percentage "change in response from baseline". Data were statistically compared using Prism 7 software (GraphPad Software, San Diego, CA, USA), and where appropriate, were analysed using a one or two-way analysis of variance (ANOVA) with Bonferroni post hoc tests. Differences were considered significant at a level of * $P < 0.05$, ** $P < 0.01$, *** $P < 0.001$ and **** $P < 0.0001$. *n* = the number of afferents. N = the number of animals.

**Supporting information:** Includes additional electrophysiology data, NMR chemical shift tables, and structure statistics for cVc1.1[D11A,E14A]. This material is available free of charge via the internet at http://pubs.acs.org

**Acknowledgements**: This work was funded by the National Health and Medical Research Council (NHMRC) of Australia Project Grant #1049928 awarded to D.J.A, S.M.B and D.J.C. S.M.B is an NHMRC R.D Wright Biomedical Research Fellow (APP1126378). R.J.C. received funding via an ARC Future Fellowship (FT100100476) and D.J.C. is an ARC Australian Laureate Fellow (FL150100146).

**Author contributions:** MS performed research, analysed data and wrote the paper; BPC performed research and analysed data; JTD performed research, analysed data and wrote the paper; HT performed research and analysed data; JC performed research and analysed data; TO'D performed research and analysed data; SMB, DJA and DJC designed research and wrote the paper; RJC designed research, performed research, analysed data and wrote the paper.

**Competing Financial Interests and Conflict of Interests:** The authors have no competing interests or conflict of interests.

## References

1. Bowery, N. G., Hill, D. R., Hudson, A. L., Doble, A., Middlemiss, D. N., Shaw, J., and Turnbull, M. (1980) (-)Baclofen decreases neurotransmitter release in the mammalian CNS by an action at a novel GABA receptor, *Nature 283*, 92-94.

2. Hill, D. R., and Bowery, N. G. (1981) 3H-baclofen and 3H-GABA bind to bicuculline-insensitive GABA B sites in rat brain, *Nature 290*, 149-152.

3. Pinard, A., Seddik, R., and Bettler, B. (2010) GABAB receptors: physiological functions and mechanisms of diversity, *Adv. Pharmacol. 58*, 231-255.

4. Brauner-Osborne, H., Wellendorph, P., and Jensen, A. A. (2007) Structure, pharmacology and therapeutic prospects of family C G-protein coupled receptors, *Curr. Drug Targets 8*, 169-184.

5. Dunlap, K., and Fischbach, G. D. (1981) Neurotransmitters decrease the calcium conductance activated by depolarization of embryonic chick sensory neurones, *J. Physiol. 317*, 519-535.

6. Catterall, W. A., and Few, A. P. (2008) Calcium channel regulation and presynaptic plasticity, *Neuron 59*, 882-901.

7. Stephens, G. J. (2009) G-protein-coupled-receptor-mediated presynaptic inhibition in the cerebellum, *Trends Pharmacol. Sci. 30*, 421-430.

8. Altier, C., and Zamponi, G. W. (2004) Targeting Ca2+ channels to treat pain: T-type versus N-type, *Trends Pharmacol. Sci. 25*, 465-470.

9. Sandall, D. W., Satkunanathan, N., Keays, D. A., Polidano, M. A., Liping, X., Pham, V., Down, J. G., Khalil, Z., Livett, B. G., and Gayler, K. R. (2003) A novel alpha-conotoxin identified by gene sequencing is active in suppressing the

vascular response to selective stimulation of sensory nerves in vivo, *Biochemistry 42*, 6904-6911.

10. Clark, R. J., Fischer, H., Nevin, S. T., Adams, D. J., and Craik, D. J. (2006) The synthesis, structural characterization, and receptor specificity of the alpha-conotoxin Vc1.1, *J. Biol. Chem. 281*, 23254-23263.
11. Vincler, M., Wittenauer, S., Parker, R., Ellison, M., Olivera, B. M., and McIntosh, J. M. (2006) Molecular mechanism for analgesia involving specific antagonism of alpha9alpha10 nicotinic acetylcholine receptors, *Proc. Natl. Acad. Sci. U. S. A. 103*, 17880-17884.
12. Ellison, M., Haberlandt, C., Gomez-Casati, M. E., Watkins, M., Elgoyhen, A. B., McIntosh, J. M., and Olivera, B. M. (2006) alpha-RgIA: A novel conotoxin that specifically and potently blocks the alpha 9 alpha 10 nAChR, *Biochemistry 45*, 1511-1517.
13. Callaghan, B., Haythornthwaite, A., Berecki, G., Clark, R. J., Craik, D. J., and Adams, D. J. (2008) Analgesic alpha-conotoxins Vc1.1 and Rg1A inhibit N-type calcium channels in rat sensory neurons via GABAB receptor activation, *J. Neurosci. 28*, 10943-10951.
14. Cuny, H., de Faoite, A., Huynh, T. G., Yasuda, T., Berecki, G., and Adams, D. J. (2012) gamma-Aminobutyric acid type B (GABAB) receptor expression is needed for inhibition of N-type (Cav2.2) calcium channels by analgesic alpha-conotoxins, *J. Biol. Chem. 287*, 23948-23957.
15. Berecki, G., McArthur, J. R., Cuny, H., Clark, R. J., and Adams, D. J. (2014) Differential Cav2.1 and Cav2.3 channel inhibition by baclofen and alpha-conotoxin Vc1.1 via GABAB receptor activation, *J. Gen. Physiol. 143*, 465-479.

16. Daly, N. L., Callaghan, B., Clark, R. J., Nevin, S. T., Adams, D. J., and Craik, D. J. (2011) Structure and activity of alpha-conotoxin PeIA at nicotinic acetylcholine receptor subtypes and GABAB receptor-coupled N-type calcium channels, *J. Biol. Chem. 286*, 10233-10237.

17. Safavi-Hemami, H., Siero, W. A., Kuang, Z., Williamson, N. A., Karas, J. A., Page, L. R., MacMillan, D., Callaghan, B., Kompella, S. N., Adams, D. J., Norton, R. S., and Purcell, A. W. (2011) Embryonic toxin expression in the cone snail *Conus victoriae*: primed to kill or divergent function?, *J. Biol. Chem. 286*, 22546-22557.

18. Carstens, B. B., Berecki, G., Daniel, J. T., Lee, H. S., Jackson, K. A., Tae, H. S., Sadeghi, M., Castro, J., O'Donnell, T., Deiteren, A., Brierley, S. M., Craik, D. J., Adams, D. J., and Clark, R. J. (2016) Structure-Activity Studies of Cysteine-Rich alpha-Conotoxins that Inhibit High-Voltage-Activated Calcium Channels via GABAB Receptor Activation Reveal a Minimal Functional Motif, *Angew. Chem. Int. Ed. Engl. 55*, 4692-4696.

19. Klimis, H., Adams, D. J., Callaghan, B., Nevin, S., Alewood, P. F., Vaughan, C. W., Mozar, C. A., and Christie, M. J. (2011) A novel mechanism of inhibition of high-voltage activated calcium channels by alpha-conotoxins contributes to relief of nerve injury-induced neuropathic pain, *Pain 152*, 259-266.

20. Nevin, S. T., Clark, R. J., Klimis, H., Christie, M. J., Craik, D. J., and Adams, D. J. (2007) Are alpha9alpha10 nicotinic acetylcholine receptors a pain target for alpha-conotoxins?, *Mol. Pharmacol. 72*, 1406-1410.

21. Castro, J., Harrington, A. M., Garcia-Caraballo, S., Maddern, J., Grundy, L., Zhang, J., Page, G., Miller, P. E., Craik, D. J., Adams, D. J., and Brierley, S. M.

(2016) α-conotoxin Vc1.1 inhibits human dorsal root ganglion neuroexcitability and mouse colonic nociception via GABAB receptors., *Gut 66*, 1083-1094.

22. Clark, R. J., Jensen, J., Nevin, S. T., Callaghan, B. P., Adams, D. J., and Craik, D. J. (2010) The engineering of an orally active conotoxin for the treatment of neuropathic pain, *Angew. Chem. Int. Ed. Engl. 49*, 6545-6548.
23. Romero, H. K., Christensen, S. B., Di Cesare Mannelli, L., Gajewiak, J., Ramachandra, R., Elmslie, K. S., Vetter, D. E., Ghelardini, C., Iadonato, S. P., Mercado, J. L., Olivera, B. M., and McIntosh, J. M. (2017) Inhibition of alpha9alpha10 nicotinic acetylcholine receptors prevents chemotherapy-induced neuropathic pain, *Proc. Natl. Acad. Sci. U. S. A. 114*, E1825-E1832.
24. Wala, E. P., Crooks, P. A., McIntosh, J. M., and Holtman, J. R., Jr. (2012) Novel small molecule alpha9alpha10 nicotinic receptor antagonist prevents and reverses chemotherapy-evoked neuropathic pain in rats, *Anesth. Analg. 115*, 713-720.
25. Holtman, J. R., Dwoskin, L. P., Dowell, C., Wala, E. P., Zhang, Z., Crooks, P. A., and McIntosh, J. M. (2011) The novel small molecule alpha9alpha10 nicotinic acetylcholine receptor antagonist ZZ-204G is analgesic, *Eur. J. Pharmacol. 670*, 500-508.
26. Halai, R., Clark, R. J., Nevin, S. T., Jensen, J. E., Adams, D. J., and Craik, D. J. (2009) Scanning mutagenesis of alpha-conotoxin Vc1.1 reveals residues crucial for activity at the alpha9alpha10 nicotinic acetylcholine receptor, *J. Biol. Chem. 284*, 20275-20284.
27. Yu, R., Kompella, S. N., Adams, D. J., Craik, D. J., and Kaas, Q. (2013) Determination of the alpha-conotoxin Vc1.1 binding site on the alpha9alpha10 nicotinic acetylcholine receptor, *J. Med. Chem. 56*, 3557-3567.

28. Ellison, M., Feng, Z. P., Park, A. J., Zhang, X., Olivera, B. M., McIntosh, J. M., and Norton, R. S. (2008) Alpha-RgIA, a novel conotoxin that blocks the alpha9alpha10 nAChR: structure and identification of key receptor-binding residues, *J. Mol. Biol. 377*, 1216-1227.

29. Armishaw, C. J., Banerjee, J., Ganno, M. L., Reilley, K. J., Eans, S. O., Mizrachi, E., Gyanda, R., Hoot, M. R., Houghten, R. A., and McLaughlin, J. P. (2013) Discovery of novel antinociceptive alpha-conotoxin analogues from the direct in vivo screening of a synthetic mixture-based combinatorial library, *ACS Comb Sci 15*, 153-161.

30. Azam, L., Papakyriakou, A., Zouridakis, M., Giastas, P., Tzartos, S. J., and McIntosh, J. M. (2015) Molecular interaction of alpha-conotoxin RgIA with the rat alpha9alpha10 nicotinic acetylcholine receptor, *Mol. Pharmacol. 87*, 855-864.

31. Clark, J., Jensen, J., Nevin, S., Brid, C., Adams, D., and Craik, D. (2010) The Engineering of an Orally Active Conotoxin for the Treatment of Neuropathic Pain, *J. Pept. Sci. 16*, 45-45.

32. Güntert, P., Mumenthaler, C., and Wüthrich, K. (1997) Torsion angle dynamics for NMR structure calculation with the new program DYANA, *J. Mol. Biol. 273*, 283-298.

33. Shen, Y., Delaglio, F., Cornilescu, G., and Bax, A. (2009) TALOS+: a hybrid method for predicting protein backbone torsion angles from NMR chemical shifts, *J. Biomol. NMR 44*, 213-223.

34. Lovelace, E. S., Gunasekera, S., Alvarmo, C., Clark, R. J., Nevin, S. T., Grishin, A. A., Adams, D. J., Craik, D. J., and Daly, N. L. (2011) Stabilization of alpha-conotoxin AuIB: influences of disulfide connectivity and backbone cyclization, *Antioxid. Redox Signal. 14*, 87-95.

35. Castro, J., Grundy, L., Deiteren, A., Harrington, A. M., O'Donnell, T., Maddern, J., Moore, J., Garcia-Caraballo, S., Rychkov, G. Y., Yu, R., Kaas, Q., Craik, D. J., Adams, D. J., and Brierley, S. M. (2017) Cyclic analogues of alpha-conotoxin Vc1.1 inhibit colonic nociceptors and provide analgesia in a mouse model of chronic abdominal pain, *Br. J. Pharmacol. doi: 10.1111/bph.14115*.

36. Schnölzer, M., Alewood, P., Jones, A., Alewood, D., and Kent, S. B. H. (1992) *In situ* neutralization in Boc-chemistry solid phase peptide synthesis., *Int. J. Pept. Protein Res. 40*, 180-193.

37. Dawson, P. E., Muir, T. W., Clark-Lewis, I., and Kent, S. B. (1994) Synthesis of proteins by native chemical ligation, *Science 266*, 776-779.

38. Callaghan, B., and Adams, D. J. (2010) Analgesic alpha-conotoxins Vc1.1 and RgIA inhibit N-type calcium channels in sensory neurons of alpha9 nicotinic receptor knockout mice, *Channels 4*, 1-4.

39. Castro, J., Harrington, A. M., Hughes, P. A., Martin, C. M., Ge, P., Shea, C. M., Jin, H., Jacobson, S., Hannig, G., Mann, E., Cohen, M. B., MacDougall, J. E., Lavins, B. J., Kurtz, C. B., Silos-Santiago, I., Johnston, J. M., Currie, M. G., Blackshaw, L. A., and Brierley, S. M. (2013) Linaclotide inhibits colonic nociceptors and relieves abdominal pain via guanylate cyclase-C and extracellular cyclic guanosine 3',5'-monophosphate, *Gastroenterology 145*, 1334-1346 e1331-1311.

40. de Araujo, A. D., Mobli, M., Castro, J., Harrington, A. M., Vetter, I., Dekan, Z., Muttenthaler, M., Wan, J., Lewis, R. J., King, G. F., Brierley, S. M., and Alewood, P. F. (2014) Selenoether oxytocin analogues have analgesic properties in a mouse model of chronic abdominal pain, *Nat Commun 5*, 3165.

41. Hughes, P. A., Brierley, S. M., Martin, C. M., Brookes, S. J., Linden, D. R., and Blackshaw, L. A. (2009) Post-inflammatory colonic afferent sensitisation: different subtypes, different pathways and different time courses, *Gut 58*, 1333-1341.

42. Hughes, P. A., Castro, J., Harrington, A. M., Isaacs, N., Moretta, M., Hicks, G. A., Urso, D. M., and Brierley, S. M. (2014) Increased kappa-opioid receptor expression and function during chronic visceral hypersensitivity, *Gut 63*, 1199-1200.

43. Osteen, J. D., Herzig, V., Gilchrist, J., Emrick, J. J., Zhang, C., Wang, X., Castro, J., Garcia-Caraballo, S., Grundy, L., Rychkov, G. Y., Weyer, A. D., Dekan, Z., Undheim, E. A., Alewood, P., Stucky, C. L., Brierley, S. M., Basbaum, A. I., Bosmans, F., King, G. F., and Julius, D. (2016) Selective spider toxins reveal a role for the Nav1.1 channel in mechanical pain, *Nature 534*, 494-499.

44. Harrington, A. M., Brierley, S. M., Isaacs, N., Hughes, P. A., Castro, J., and Blackshaw, L. A. (2012) Sprouting of colonic afferent central terminals and increased spinal mitogen-activated protein kinase expression in a mouse model of chronic visceral hypersensitivity, *J. Comp. Neurol. 520*, 2241-2255.

45. Adam, B., Liebregts, T., Gschossmann, J. M., Krippner, C., Scholl, F., Ruwe, M., and Holtmann, G. (2006) Severity of mucosal inflammation as a predictor for alterations of visceral sensory function in a rat model, *Pain 123*, 179-186.

46. Brierley, S. M., Jones, R. C., 3rd, Gebhart, G. F., and Blackshaw, L. A. (2004) Splanchnic and pelvic mechanosensory afferents signal different qualities of colonic stimuli in mice, *Gastroenterology 127*, 166-178.

47. Brierley, S. M., Jones, R. C., 3rd, Xu, L., Gebhart, G. F., and Blackshaw, L. A. (2005) Activation of splanchnic and pelvic colonic afferents by bradykinin in mice, *Neurogastroenterol. Motil. 17*, 854-862.

48. Hughes, P. A., Harrington, A. M., Castro, J., Liebregts, T., Adam, B., Grasby, D. J., Isaacs, N. J., Maldeniya, L., Martin, C. M., Persson, J., Andrews, J. M., Holtmann, G., Blackshaw, L. A., and Brierley, S. M. (2013) Sensory neuro-immune interactions differ between irritable bowel syndrome subtypes, *Gut 62*, 1456-1465.

49. Brierley, S. M., Hughes, P. A., Page, A. J., Kwan, K. Y., Martin, C. M., O'Donnell, T. A., Cooper, N. J., Harrington, A. M., Adam, B., Liebregts, T., Holtmann, G., Corey, D. P., Rychkov, G. Y., and Blackshaw, L. A. (2009) The ion channel TRPA1 is required for normal mechanosensation and is modulated by algesic stimuli, *Gastroenterology 137*, 2084-2095 e2083.

50. Brierley, S. M., Castro, J., Harrington, A. M., Hughes, P. A., Page, A. J., Rychkov, G. Y., and Blackshaw, L. A. (2011) TRPA1 contributes to specific mechanically activated currents and sensory neuron mechanical hypersensitivity, *J. Physiol. 589*, 3575-3593.

51. Brierley, S. M., Page, A. J., Hughes, P. A., Adam, B., Liebregts, T., Cooper, N. J., Holtmann, G., Liedtke, W., and Blackshaw, L. A. (2008) Selective role for TRPV4 ion channels in visceral sensory pathways, *Gastroenterology 134*, 2059-2069.

**Figure legends**

**Figure 1**. Vc1.1 and other α-conotoxins that inhibit HVA calcium channels via activation of the $GABA_BR$. (**a**) The sequence and three dimensional structure of Vc1.1. The peptide consists of 16 amino acids containing four cysteine residues that form two disulfide bonds in a Cys2-Cys8 and Cys3-Cys16 pattern. The "loop" regions of the peptide are defined as the sequences between Cys3 and Cys8 (Loop 1, shown in orange) and Cys8 and Cys16 (Loop 2, shown in blue). These loops vary in length and composition between different α-conotoxins and confer affinity and specifity for their molecular targets. Vc1.1 adopts the archetypal three dimensional structure of α-conotoxins, which consists of a helical region stabilised by the two disulfide bonds. (**b**) Sequences and biological activity data for α-conotoxins that exhibit HVA calcium channel inhibitory activity. There is significant loop sequence variation between these α-conotoxins and it is difficult to extrapolate any clear structure/activity relationships. Activity data for the peptides is from the following articles: Vc1.1,[13] Vc1.2,[17] RgIA,[13] AuIB,[19] PeIA,[16] Pu1.2,[18] Pn1.2,[18] Kn1.2[18] and Tx1.2.[18]

**Figure 2.** Effect of Vc1.1 point mutation analogues (100 nM) on HVA calcium channel currents in mouse DRG neurons. (**a**-**c**) Bar graphs of the inhibition of HVA calcium channels current by alanine (**a**), aspartic acid (**b**) or lysine (**c**) substituted analogues of Vc1.1. Loop regions are highlighted by the dotted lines and grey horizontal bars. The *asterisk* indicates mutants with significantly decreased potency relative to Vc1.1 (unpaired student t test.($p < 0.05$)). Only G1A, G1D, S4D, S4K, N9D, N9K, D11A, D11K, E14A, E14D, I15A, and I15D retain activity at $GABA_BR$-mediated inhibition of HVA calcium channels from DRG neurons. Dotted line

indicate the level of $I/I_{Ba}$ inhibition by Vc1.1. There was a significant differences between Vc1.1 and baclofen (50 μM) ($p < 0.0001$). The number of experiments, n, is in parentheses. Data points are mean ± SEM. (**d**) A summary of the substitutions that lead to changes in the activity of Vc1.1. The sequence of Vc1.1 is shown in black and white with the disulfide bonds highlighted by black lines. The red circles represent substitutions that lead to loss of activity, the yellow circles represent mutations with comparable activity to Vc1.1, and the green circles represent substitutions that lead to an increase in potency. The structure-activity summary for the $GABA_BR$-mediated inhibition of HVA calcium currents is shown above the native Vc1.1 sequence. The mutational study data for inhibition of rα9α10 nAChRs, described previously by Halai et al.,[26] is summarized below the sequence of Vc1.1.

**Figure 3.** Three dimensional solution structure of cVc1.1[D11A,E14A] and its comparison to cVc1.1. **(a)** NMR ensemble of the twenty lowest energy structures of cVc1.1[D11A,E14A] superimposed over the backbone atoms of Gly1 to Cys16 (highlighted in green). The linker sequence is shown in grey and the disulfide bonds are shown in yellow. **(b)** The lowest energy structure of cVc1.1[D11A,E14A] represented in ribbon style, with disulfide bonds shown as balls and sticks. The peptide secondary structure comprises an α-helical region from Pro6 to Ala11, which is consistent with the structure of Vc1.1 and other α-conotoxins, and second short helix in the linker region (Gly18 to Ala21). **(c)** Surface representation of cVc1.1[D11A,E14A] (top) and cVc1.1 (bottom). Hydrophobic residues are shaded in green, polar uncharged in grey, negatively charged in red, positively charged in blue, glycine in cyan and cystines in yellow. The major difference in surface features is the absence of the negatively charged patch in cVc1.1[D11A, E14A] (top right), which is

formed by Asp11 and Glu14 in cVc1.1 (bottom right). **(d)** Comparison of the backbone conformations of cVc1.1[D11A,E14A] (green) and cVc1.1 (blue). The lowest energy structure of cVc1.1[D11A,E14A] and cVc1.1 are shown superimposed over the backbone atoms of Cys2 to Ile15 (RMSD = 0.68 Å). Disulfide bonds are shown in yellow and orange for cVc1.1[D11A,E14A] and cVc1.1, respectively. Linker regions are shown in grey.

**Figure 4**. (**a**) Inhibition of HVA calcium channel current in DRG neurons by Vc1.1[D11A,E14A] and cVc1.1[D11A,E14A]. **(i)** Superimposed representative time plots showing inhibition of peak $I_{Ba}$ by 100 nM Vc1.1[D11A,E14A] (left), 100 nM cVc1.1[D11A,E14A] (right) and 50 μM baclofen in mouse DRG neurons. Bars indicate the duration of peptide or baclofen application. Inward $I_{Ba}$ were evoked by voltage steps, from a HP of −80 mV to 5 or 0 mV applied at 0.1 Hz, respectively (*insets*). Superimposed representative $I_{Ba}$ traces (*insets*) obtained in the absence (a) and presence of peptide (b), and 50 μM baclofen (c), are shown at the times indicated by lowercase letters. Dotted lines indicate zero-current level. **(ii)** Bar graph summary of data on inhibition of $Ba^{2+}$ peak amplitude by 100 nM Vc1.1, Vc1.1[D11A,E14A], cVc1.1, cVc1.1[D11A,E14A], and baclofen (50 μM). Data are presented as mean ± SEM, asterisks indicate statistically significant differences versus Vc1.1 (* $P < 0.05$ and *** $P < 0.001$; one-way ANOVA). The number of experiments, *n*, is in parentheses. **(iii)** Concentration-response curve for inhibition of HVA calcium channel currents in rat DRG neurons by Vc1.1[D11A,E14A] (open squares, $IC_{50}$ of 2.5 ± 1.0 nM, $n$ = 4-7) and cVc1.1[D11A,E14A] (open circles, 3.3 ± 1.1 nM, $n$ = 4-9). Data points are mean ± SEM. **(b)** Inhibition of human(h) α9α10 nAChRs expressed in *Xenopus* oocytes by Vc1.1, Vc1.1[D11A,E14A], cVc1.1 and cVc1.1[D11A,E14A]. **(i)**

Superimposed representative ACh (6 μM)-evoked currents mediated by hα9α10 nAChRs in the absence (black) and presence (red) of 1 μM Vc1.1, Vc1.1[D11A,E14A], cVc1.1, or cVc1.1[D11A,E14A]. **(ii)** Bar graph of 1 μM Vc1.1, Vc1.1[D11A,E14A], cVc1.1 or cVc1.1[D11A,E14A] inhibition of ACh-evoked peak current amplitude mediated by hα9α10 nAChRs. **(iii)** Concentration-response relationships for Vc1.1[D11A,E14A] (open squares) and cVc1.1[D11A,E14A] (open circles) inhibition of ACh-evoked current amplitude giving $IC_{50}$'s of 9.2 ± 1.3 μM and 29.3 ± 3.0 μM, respectively. Current amplitudes (mean ± SEM, $n$ = 4-9) were normalized to the response elicted by 6 μM ACh (corresponding to the $EC_{50}$ value at hα9α10 nAChRs).

**Figure 5.** cVc1.1[D11A,E14A] inhibits the mechanosensitivity of colonic nociceptors from healthy and CVH mice. **(a)** Healthy colonic nociceptor mechanosensitivity is significantly reduced following increasing concentrations of cVc1.1[D11A,E14A], with significant reductions compared with baseline observed at 10 nM (* $P$<0.05), 100 nM (** $P$<0.01) and 1 μM (** $P$<0.01. (n = 6 afferents, one-way ANOVA, Bonferroni-*posthoc*). **(b)** In colonic nociceptors from CVH mice, cVc1.1[D11A,E14A] potently and concentration-dependently inhibited CVH nociceptors at 10 nM (***$P$<0.001), 100 nM (****$P$<0.0001) and 1000 nM (****$P$<0.0001; n = 5 afferents, one-way ANOVA, Bonferroni-*posthoc*). **(c)** Change in mechanosensitivity, expressed as spikes/sec from baseline, induced by [D11A,D14A] cVc1.1 in healthy and CVH nociceptors compared with their respective baseline responses. cVc1.1[D11A,E14A] caused significantly more inhibition at 10 nM (* $P$<0.001), 100 nM (**** $P$<0.0001), and 1 μM (**** $P$<0.0001) in CVH nociceptors compared with healthy nociceptors ($n$ = 6 healthy, $n$ =

5 CVH, two-way ANOVA, Bonferroni *posthoc*). **(d)** Original recordings of a healthy colonic nociceptor, showing action potential firing in response to a 2 g vfh probe at baseline and in the presence of cVc1.1[D11A,E14A] (1000 nM). **(e)** Original recordings of a CVH colonic nociceptor showing action potential firing in response to a 2 g vfh probe at baseline and in the presence of cVc1.1[D11A,E14A] (1000 nM). **(f).** Percentage of colonic nociceptor inhibition induced by cVc1.1 in response to mechanical stimulation in healthy and CVH states. Data modified from Castro *et al.*.[20] **(g).** Percentage of colonic nociceptor inhibition induced by cVc1.1[D11A,E14A] in response to mechanical stimulation in healthy and CVH states. These data show that cVc1.1[D11A,E14A] evoked greater inhibition of colonic nociceptors in CVH states, cuasing greater inhibition at 100 nM (** $P<0.01$) and 1000 nM (** $P<0.01$). **(h).** Comparative inhibitory effect of cVc1.1 and cVc1.1[D11A,E14A] on colonic nociceptor mechanosensitivity in healthy states. cVc1.1 data modified from Castro *et al.*.[35] **(i).** Comparative inhibitory effect of cVc1.1 and cVc1.1[D11A,E14A] on colonic nociceptor mechanosensitivity in CVH states. cVc1.1 data modified from Castro *et al.*.[35]

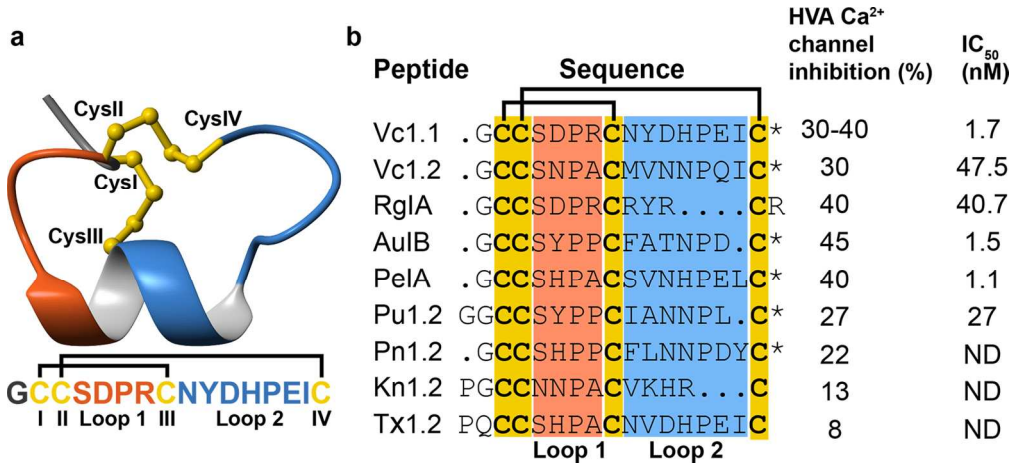


Figure 1

140x63mm (300 x 300 DPI)

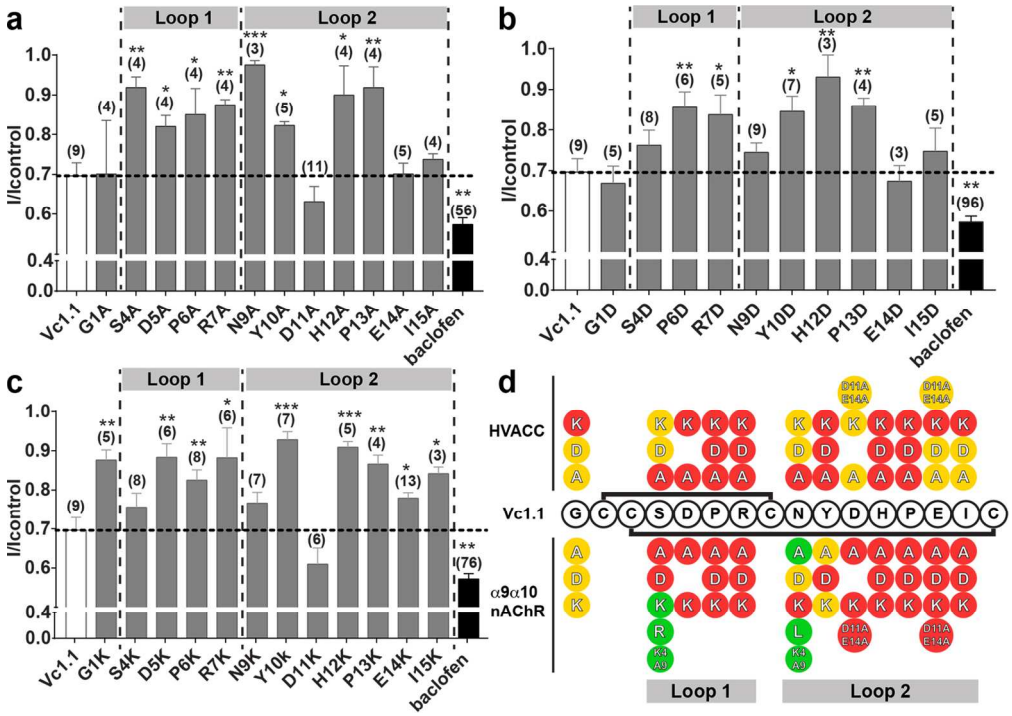


Figure 2

140x98mm (300 x 300 DPI)

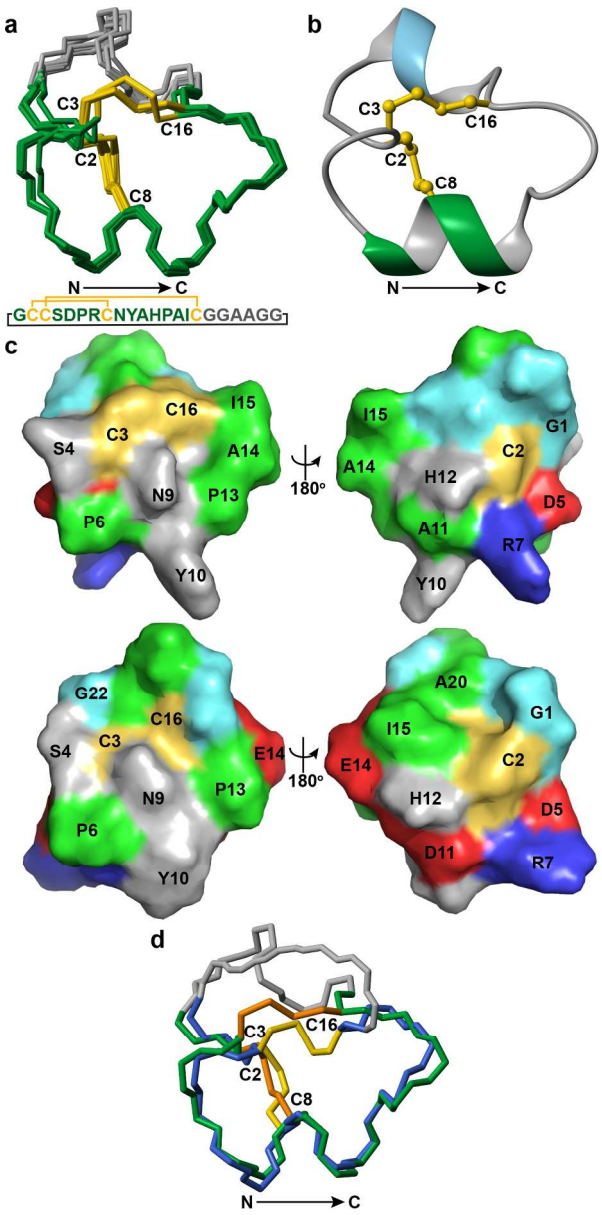


Figure 3

118x240mm (300 x 300 DPI)

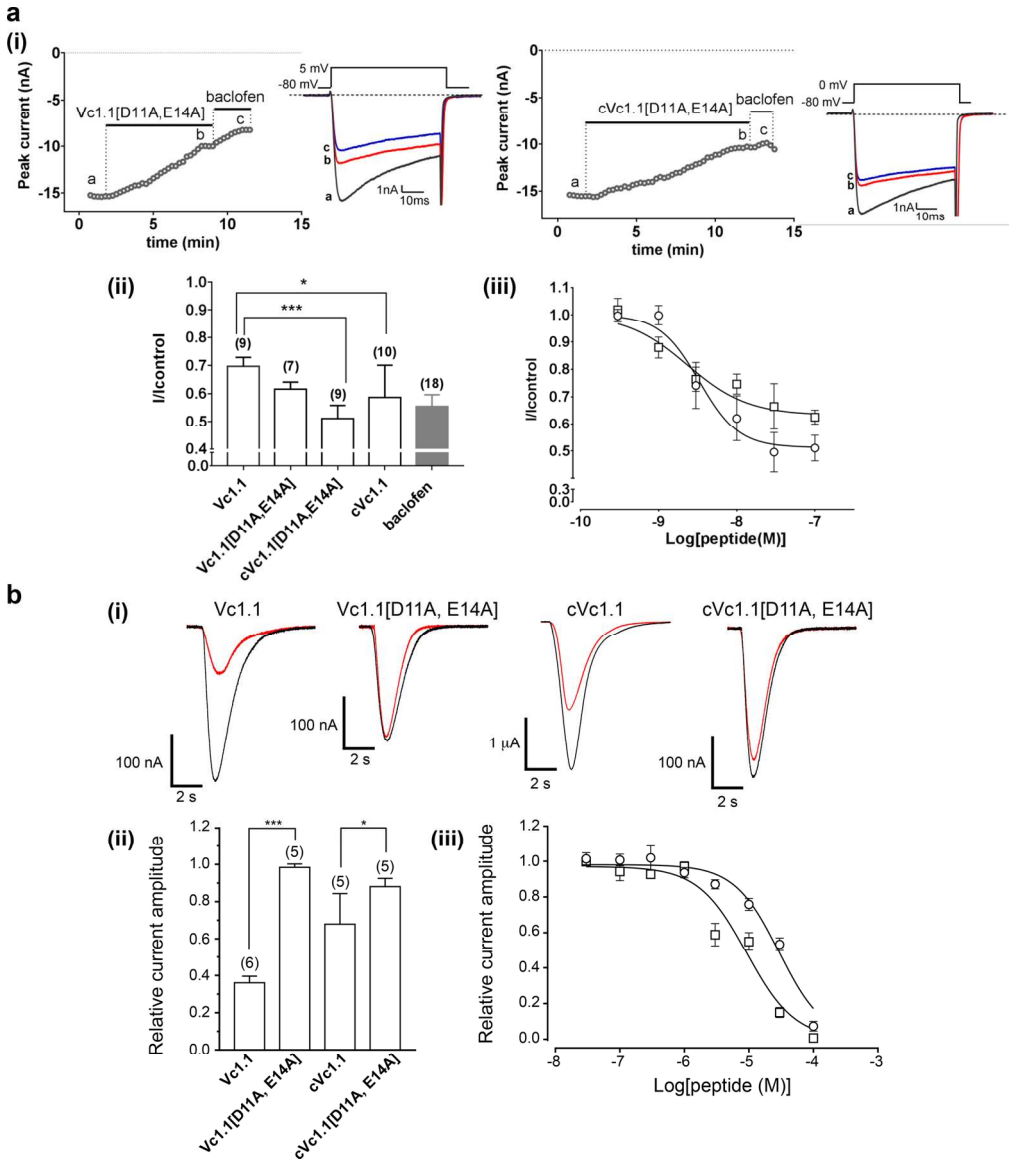


Figure 4

160x184mm (300 x 300 DPI)

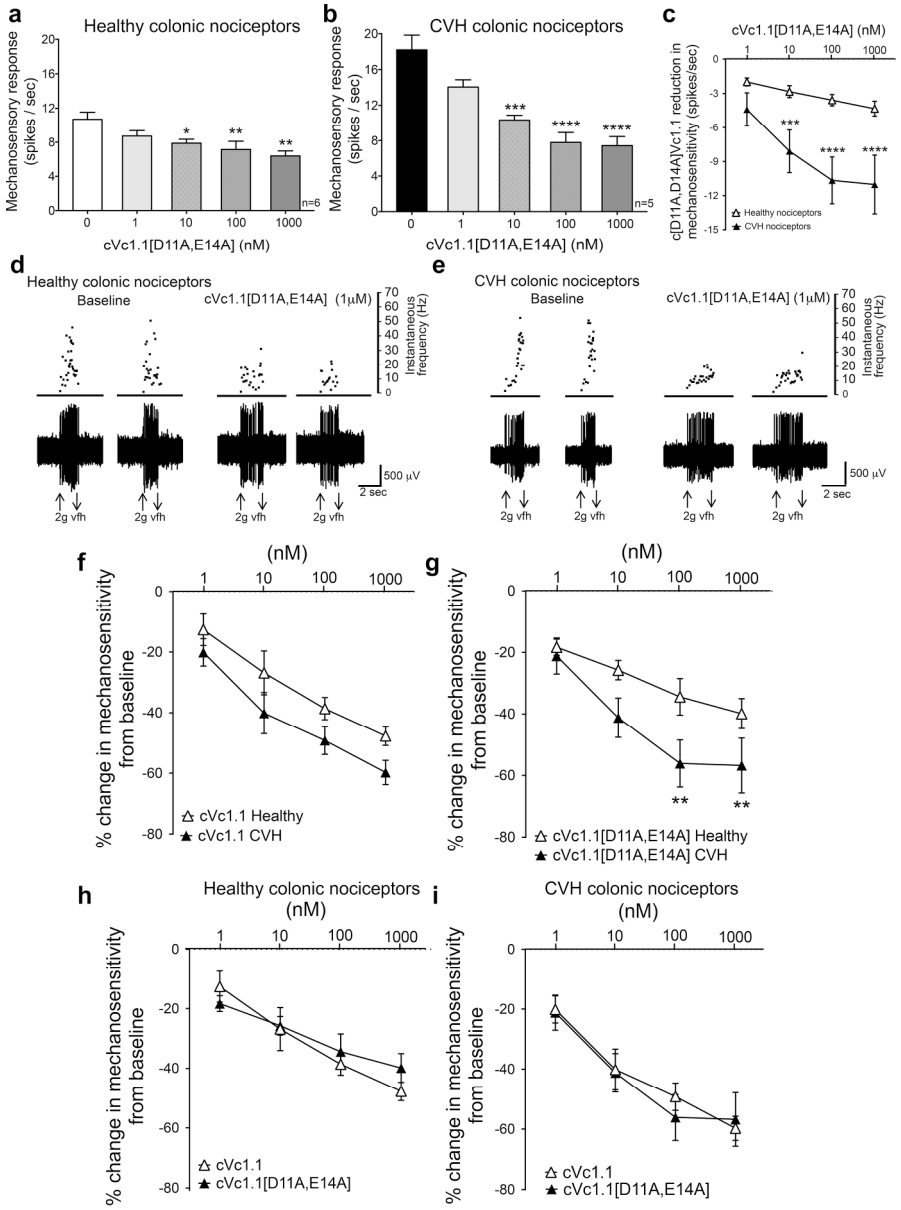


Figure 5

188x254mm (300 x 300 DPI)

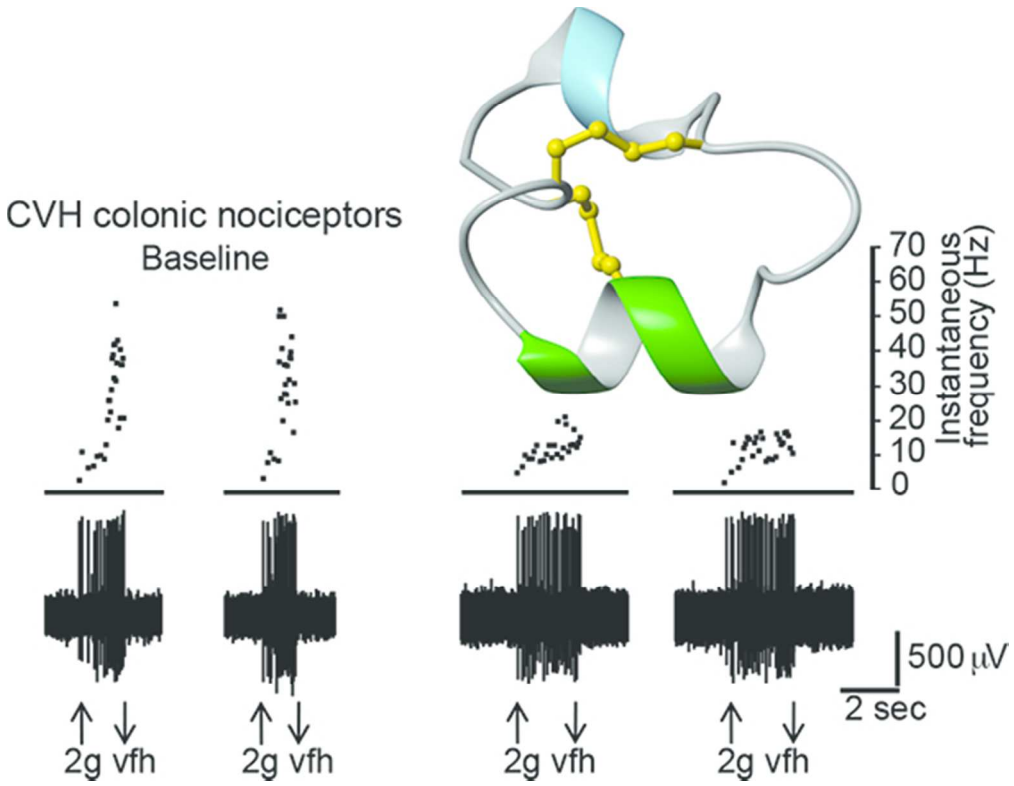


Table of Contents Graphic

51x39mm (300 x 300 DPI)